Structural differences in two polymorphs of tetra-*kis*-(dimethylamino)-ethylene-C$_{60}$: An x-ray diffraction study

Motoyasu Fujiwara, Takashi Kambe,* and Kokichi Oshima

Graduate School of Natural Science and Technology, Okayama University, 3-1-1 Tsushimanaka, Okayama 700-8530, Japan

(Received 22 October 2004; revised manuscript received 24 February 2005; published 25 May 2005)

A type of low-temperature structure for ferromagnetic α-tetra-*kis* (dimethylamino)-ethylene (TDAE)-C$_{60}$ is proposed on the basis of low-temperature x-ray analysis. We observed that intense superlattice reflections with odd indices successively appeared below $T_s = 170$ K. The space group symmetry of the low-temperature phase is determined to be $P2_1/n$. Two inequivalent C$_{60}$ sites exist in the low-temperature phase, which are indispensable to the orbital ordering model of C$_{60}$. The contact configuration for the neighboring C$_{60}$s along the stacking c direction is uniquely determined. The double bond between the hexagons faces the neighboring pentagon. We found that the surrounding TDAE molecules shift along the c axis (~ 0.07 Å) and that these shifts correlate perfectly to the alignment of C$_{60}$. This result indicates that the steric effect between C$_{60}$ and TDAE molecules plays an important role in the orientational ordering of C$_{60}$. On the other hand, in the α' phase, no structural phase transition was observed below 30 K. This indicates that all the C$_{60}$s are crystallographically equivalent. Structural differences separate the magnetic peculiarities of the two polymorphs in TDAE-C$_{60}$.

I. INTRODUCTION

Molecular magnetism, that is, the magnetic interaction between molecules, has recently attracted considerable attention. Several molecular magnets that can be classified as antiferromagnet, ferromagnet, and ferrimagnet have been systematically designed.[1] Unpaired electrons in the molecules give rise to the magnetism. The antiparallel configuration of molecular spins is usually favorable because it leads to an increase in the electron transfer energy. The sign of magnetic interaction between molecules depends on the delicate balance among the kinetic exchange term, Coulomb interaction, and spin polarization effect.

Tetra-*kis*-(dimethylamino)-ethylene (TDAE) C$_{60}$ is a fullerene ferromagnet with the highest transition temperature, $T_c = 16$ K, among organic ferromagnets.[2] Detailed ferromagnetic resonance (FMR) measurements were conducted using a single crystal,[3] and the frequency-field diagram was explained using the usual Kittel's model with an extremely weak uniaxial anisotropy. This experiment establishes that the ground state of TDAE-C$_{60}$ is the same as that of a bulk ferromagnet with the highest transition temperature among purely organic materials. It is also known that its ferromagnetism strongly depends on the annealing procedure of the samples. Following the experiment, two polymorphs were discovered in the salt: a ferromagnetic α phase and a nonferromagnetic α' phase. The α' phase crystals irreversibly transform into α-phase crystals by thermal annealing.[4] The magnetic susceptibility of the α' phase obeys a simple Curie-Weiss law at a high temperature region with a negative Weiss constant. No magnetic ordering was observed down to 1.5 K, and the nonmagnetic singlet ground state was proposed in this phase.[5] Although the mechanism of the ferromagnetic interaction in the α phase has been discussed extensively, this issue is still debatable. Several theoretical studies were conducted to explain the highest transition temperature of

this salt. Recently, Kawamoto *et al.* proposed a model with cooperative ordering of Jahn-Teller (JT) distorted C$_{60}$.[6] In this model, the orientation of the orbitals of neighboring JT-distorted C$_{60}$s cooperatively order with the orthogonal configuration of the twofold axes in order to reduce the direct overlapping between the orbitals. The electron correlation in the nearly degenerated t_{1u} orbitals would perform well for the parallel configuration of the spins of the neighboring C$_{60}$s. Experimentally, the pressure dependence of the ferromagnetic transition temperature, which was investigated by the high-pressure electron spin resonance (ESR) technique,[7,8] has been well reproduced by the orbital ordering model of JT-distorted C$_{60}$. On the contrary, in order to realize antiferrorotative orbital ordering in α-TDAE-C$_{60}$, the symmetry of the crystal structure must be simultaneously lowered by the orbital ordering of C$_{60}$; this may lead to a space group lower than that of the room-temperature structure ($C2/c$). We have already reported that a structural phase transition occurs at approximately 180 K, which is possibly due to the orientational ordering of C$_{60}$,[9] but we had not succeeded in solving the low-temperature structure. On the contrary, Narymbetov *et al.* proposed a low-temperature structure that included the orientational disorder of C$_{60}$.[10] The low-temperature structure, which guides the ferromagnetic and/or antiferromagnetic interactions, is indispensable in resolving the magnetic properties of the two polymorphs. In this study, we present the results of the x-ray analysis using several single crystals from different preparation batches. For the α-phase crystals, we have succeeded in solving the low-temperature structure without introducing the orientational disorder of C$_{60}$. The final refined factor (R factor) of our analysis has improved and it is comparable with that of the disorder model. For the low-temperature structure of the α phase, we reveal the structural phase transition along with the orientational ordering of C$_{60}$, the existence of two crystallographically inequivalent C$_{60}$ sites, the unique contact configuration be-

tween the orientationally ordered C_{60} molecules, and a slight shift of TDAE molecules along the c axis. On the contrary, the low-temperature structure of the α' phase has a different type of contact between the nearest neighboring C molecules along the c axis. We compare the low-temperature structures for the two polymorphs and discuss them in relation to the magnetic interactions.

II. EXPERIMENTAL PROCEDURES

The single crystals were obtained by the usual diffusion method.[9] The typical dimensions are $0.5 \times 0.4 \times 0.3$ mm^3. For the preparation runs, we carefully selected several crystals obtained from different sample batches. As-grown α'-phase single crystals were well annealed at approximately 70 °C in order to transform them to the ferromagnetic α phase. The details of the annealing procedure are also described in Ref. 9. Both T_c and the saturation of the magnetic moment of the α phase are consistent with the previous results. The magnetization of the single crystal was measured using a commercial superconducting quantum interference device (SQUID) magnetometer (MPMS, Quantum Design Co. Ltd). All x-ray diffraction measurements were conducted using a Rigaku RAXIS-IV imaging plate diffractometer with graphite monochromated Mo $K\alpha$ radiation. From 90 K to room temperature, a liquid nitrogen continuous flow cryostat was used. Below 90 K, a He-gas continuous flow cryostat (Helix, Oxford Cryosystems) was used. The lowest temperature used for analyzing the structure was approximately 25 K. We selected several single crystals without a twin boundary to determine the low-temperature structure. One of the experimental conditions is as follows: data were collected at each temperature to a maximum 2θ value of 54.9°. A total of 90 oscillation images were acquired, each exposed for 10 min. The data were corrected for Lorentz and polarization effects. The structure was directly solved using the SIR-97 program and expanded using Fourier techniques. Non-hydrogen atoms were refined anisotropically. Hydrogen atoms were included but not refined. The final R factors for the structural refinements were less than approximately 9%. In particular, for the α phase, the R factor at 25 K improved to $\sim$5.9% without introducing the orientational disorder of C_{60}. Moreover, to confirm whether the disorder model [10] could be reproduced with our measurement result, we have performed a structure analysis using their method. The experimental conditions for the structural determination and the lattice parameters are summarized in Table I.

III. EXPERIMENTAL RESULTS AND DISCUSSION

At first, we explain the structure of the α'-phase crystal. The lattice parameters at 25 K are summarized in Table I. The R factor for the structural determination is approximately 7.3%. The low-temperature structure retains its space group symmetry ($C2/c$). Its atomic coordinates are presented in Table II. These data of crystal refinement are consistent with the previous structural analysis.[11] Since the orientation of C_{60} is completely fixed at this temperature, the contact configuration along the c axis could be well defined, as

TABLE I. Experimental conditions for crystal structure determination and lattice parameters of the α and α' phases of TDAE-C_{60} at 25 K.

Formula	$H_{24}C_{70}N_4$	
Crystal polymorph	α	α'
Crystal dimensions (mm^3)	$0.45 \times 0.45 \times 0.13$	
Crystal system	Primitive	Monoclinic
Space group	$P2_1/n$ (#14)	$C2/c$ (#15)
a/Å	15.799(1)	15.834(1)
b/Å	12.797(1)	12.7936(5)
c/Å	19.800(1)	19.725(1)
β/°	94.788(5)	94.106(2)
V/Å^3	3989.2(5)	3985.3(4)
Z value	4	4
Total reflections measured	25 394	10 771
Unique reflections	7418	4071
Reflections used	5415 ($I > 5\sigma(I)$)	3649 ($I > 5\sigma(I)$)
Residuals R; R_w	0.059; 0.060	0.073; 0.086

shown in Fig. 1(a). We will compare the contact configurations of the α' and α phases later.

Next, using the ferromagnetic α-phase single crystals, we examined the temperature dependence of the Bragg reflections because the structural phase transition temperature has not yet been correctly determined. Figure 2 shows the temperature dependence of several reflections along with the x-ray images at various temperatures. A series of intense reflections appear below $T_s = 170$ K; however, the other Bragg reflections exhibit no remarkable anomaly in their intensities near T_s. The intense superlattice reflections have odd $h + k$ indices. The smooth evolution of these superlattice reflection intensities with cooling indicates that the phase transition is of the second order. The temperature dependence of these superlattice reflections is well described by the usual $(T_s - T)^{2\beta}$ formula. The dotted line in the figure represents the fitting curve with $T_s = 170 \pm 2$ K and $2\beta = 0.43 \pm 0.02$. These results are consistent with the previous article,[9] except for the accuracy of T_s. The violation of the extinction rules below T_s indicates that the low-temperature phase has a primitive crystal structure. Some of the intensities of these superlattice reflections are comparable with those of the Bragg reflections. Diffuse scattering can also be observed at the same reciprocal wave vector above T_s, and below T_s, the superlattice peaks have well-defined profiles within the experimental resolution limit. This is in contrast to the previous structural study.[10]

We succeeded in analyzing the crystal structure below T_s. At a temperature above T_s, the structure could not be analyzed; this is probably due to the rotation of C_{60}. The lattice constants at room temperature (RT), 90 K, and 25 K are as follows: $a = 15.925$ Å, $b = 13.090$ Å, $c = 20.013$ Å, and $\beta = 93.67°$ at RT; $a = 15.805$ Å, $b = 12.822$ Å, $c = 19.815$ Å, and $\beta = 94.491°$ at 90 K; and $a = 15.799$ Å, $b = 12.797$ Å, $c = 19.800$ Å, and $\beta = 94.788°$ at 25 K. Figure 3(a) shows the temperature dependence of the lattice constants below T_s. The thermal contraction of the b axis is remarkable; this may

TABLE II. Atomic coordinates and B_{iso}/B_{eq} for the α' phase. $B_{eq}=\frac{8}{3}\pi^2[U_{11}(aa^*)^2+U_{22}(bb^*)^2+U_{33}(cc^*)^2+2U_{12}aa^*bb^*\cos\gamma+2U_{13}aa^*cc^*\cos\beta+2U_{23}bb^*cc^*\cos\alpha]$.

Atom	x	y	z	B_{eq}
N(1)	−0.0657(2)	−0.0310(2)	0.1728(1)	0.59(5)
N(2)	0.0732(2)	0.0349(2)	0.1855(1)	0.64(5)
C(1)	0.5771(2)	−0.1335(3)	−0.1409(2)	0.64(6)
C(2)	0.5434(2)	0.0497(3)	−0.1710(2)	0.66(6)
C(3)	0.6220(2)	0.0819(3)	−0.1345(2)	0.70(6)
C(4)	0.5212(2)	−0.0559(3)	−0.1744(2)	0.63(6)
C(5)	0.5183(2)	0.2090(3)	−0.1168(2)	0.70(6)
C(6)	0.6060(2)	0.1809(3)	−0.1010(2)	0.64(6)
C(7)	0.6524(2)	−0.1019(3)	−0.1061(2)	0.67(6)
C(8)	0.5246(2)	−0.2130(3)	−0.1125(2)	0.63(6)
C(9)	0.4794(2)	0.1277(3)	−0.1600(2)	0.60(6)
C(10)	0.6752(2)	0.0081(3)	−0.1027(2)	0.66(6)
C(11)	0.4351(2)	−0.0879(3)	−0.1663(2)	0.66(6)
C(12)	0.4723(2)	0.2559(3)	−0.0667(2)	0.65(6)
C(13)	0.4365(2)	−0.1850(3)	−0.1282(2)	0.70(6)
C(14)	0.6451(2)	0.2006(3)	−0.0364(2)	0.64(6)
C(15)	0.3964(2)	0.0978(3)	−0.1522(2)	0.67(6)
C(16)	0.3734(2)	−0.0120(3)	−0.1558(2)	0.68(6)
C(17)	0.5122(2)	0.2761(3)	0.0004(2)	0.57(6)
C(18)	0.5970(2)	0.2489(3)	0.0154(2)	0.59(6)
C(19)	0.3859(2)	0.2242(3)	−0.0587(2)	0.70(6)
C(20)	0.3483(2)	0.1459(3)	−0.1007(2)	0.61(6)
C(21)	0.3765(2)	−0.2027(3)	−0.0807(2)	0.56(6)
C(22)	0.3121(2)	−0.0310(3)	−0.1056(2)	0.63(6)
C(23)	0.4502(2)	0.2578(3)	0.0496(2)	0.63(6)
C(24)	0.3714(2)	0.2254(3)	0.0132(2)	0.66(6)
C(25)	0.3137(2)	−0.1242(3)	−0.0693(2)	0.69(6)
C(26)	0.2956(2)	0.0675(3)	−0.0722(2)	0.62(6)
C(27)	0.2994(2)	−0.1233(3)	0.0030(2)	0.66(6)
C(28)	0.2816(2)	0.0684(3)	−0.0027(2)	0.76(6)
C(29)	0.3212(2)	0.1489(3)	0.0408(2)	0.70(6)
C(30)	0.2845(2)	−0.0283(3)	0.0353(2)	0.69(6)
C(31)	0.0023(2)	0.0026(3)	0.2142(2)	0.66(6)
C(32)	−0.1271(2)	−0.1045(3)	0.1970(2)	0.74(6)
C(33)	−0.0877(2)	0.0175(3)	0.1067(2)	0.85(7)
C(34)	0.1051(2)	−0.0180(3)	0.1268(2)	0.81(6)
C(35)	0.1282(2)	0.1153(3)	0.2174(2)	0.90(7)
H(1)	−0.101(4)	−0.156(5)	0.232(3)	3(1)
H(2)	−0.177(3)	−0.064(4)	0.213(3)	2(1)
H(3)	−0.147(3)	−0.150(4)	0.160(3)	2.5(10)
H(4)	−0.145(2)	0.056(3)	0.107(2)	0.2(7)
H(5)	−0.094(2)	−0.041(3)	0.066(2)	0.0(6)
H(6)	−0.038(3)	0.068(4)	0.097(2)	1.7(9)
H(7)	0.069(4)	−0.082(5)	0.108(3)	3(1)
H(8)	0.112(4)	0.038(5)	0.087(3)	4(1)
H(9)	0.166(3)	−0.049(4)	0.139(2)	2.2(9)

TABLE II. (*Continued.*)

Atom	x	y	z	B_{eq}
H(10)	0.145(3)	0.162(4)	0.182(2)	1.3(8)
H(11)	0.189(3)	0.081(3)	0.242(2)	1.4(8)
H(12)	0.092(3)	0.163(4)	0.250(3)	2.4(10)

be because this direction is approximately parallel to the normal to the TDAEs molecular plane. The space group for the low-temperature phase is determined to be a primitive $P2_1/n$ one. In contrast to the previous structural analysis,[10] we succeeded in solving the low-temperature structure without assuming the orientational disorder of C_{60} molecules. The R factor for the structural analysis at 25 K improved to 5.9%. It should be noted that this value is comparable to that obtained by the model including the orientational disorder. During the experiments (approximately 10 h), the intensities of the superlattice peaks varied slightly at the lowest temperature, and the obtained results were found to be valid. Moreover, during our analyses, no additional Fourier peaks, which would suggest the existence of disorder, were observed. Figure 3(b) shows the temperature dependence of the isotropic equivalent temperature factors B_{eq} averaged over the atoms of molecules. The temperature factors rapidly decrease with cooling, except for the proton atoms. The large temperature factor of the proton atoms suggests the orientational disorder of the terminal metyl groups of the TDAE molecule. At 25 K, however, no remarkable differences in the temperature factors for the individual molecules were observed. Therefore, we conclude that it is unnecessary to consider the orientational disorder of C_{60} and that the intrinsic low-temperature structure, which guides the ferromagnetic interactions, can be determined. Tables III and IV show the atomic coordinates of the C_{60} and TDAE molecules. It should be noted that the low-temperature unit cell includes two crystallographically inequivalent C_{60} molecules. They are placed on sites 2*c* and 2*d*. This is in contrast to the case of the α' phase, which has identical C_{60} sites. In the present analysis, as C_{60} exhibits no orientational disorder below T_s, the contact configuration for the neighboring C_{60} along the stacking *c* direction is uniquely determined, as shown in Fig. 2(b). The double bond between the hexagons at which the
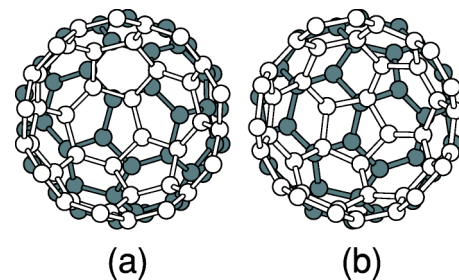

(a)   (b)

FIG. 1. Contact configuration for the nearest neighboring C_{60} viewed from the *c* axis. (a) α' phase and (b) α phase. The contact in the α' phase corresponds to the PM configuration in Fig. 3 of Ref. 10 while that in the α phase corresponds to the FM I-II configuration.
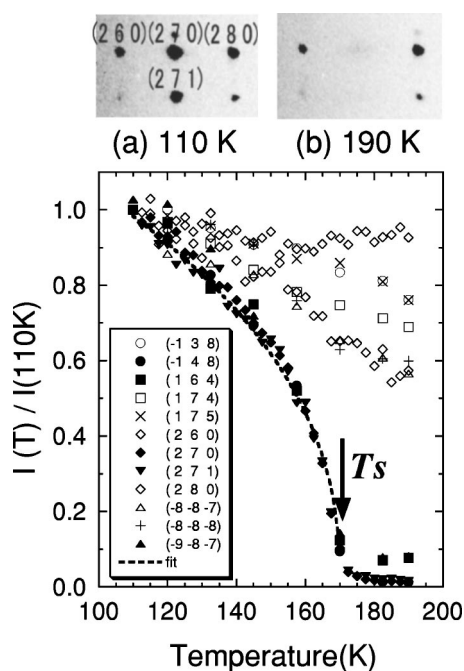
FIG. 2. Temperature dependence of the normalized intensity of reflections. Below $T_s = 170$ K, several superlattice reflections that have odd $h+k$ indices appeared. The dotted line is the fitting curve, which is described in the text. X-ray images at (a) $T = 110 < T_s$ and (b) $T = 190 > T_s$ are shown in the upper part of the figure.

twofold axis of the ball exists faces the neighboring pentagon at an angle of approximately 15° from the b axis. All the samples that were estimated, which show the ferromagnetic transition, have the same contact configuration along the c axis. This is in contrast to the contact configuration in the α' phase. At the same lowest temperature of 25 K, we could refine the structure of the α' phase. No structural phase transition was present in the α' phase. As shown in Fig. 1(a), the double bond between the hexagons faces the neighboring hexagon.

A remarkable characteristic of the low-temperature structure is that the orientation of C_{60} perfectly correlates to the shift of the surrounding TDAE molecules along the c direction. In the RT structure, the TDAE molecules are fixed at $z = 1/4$ due to the twofold axis along the b direction, but they exhibit a slight shift along the b direction. Hence, the absence of this symmetry element in the low-temperature structure allows the shift of the TDAE molecules along the c direction. Figure 4 shows the shift of the TDAE molecules, where eight TDAE molecules surround each C_{60}. The thick arrows indicate the shift directions of the TDAE molecules. In the low-temperature phase, TDAEs are placed on (~ 0, ~ 0.003, and $0.25 \pm \delta z$) with $\delta z = 0.004$ (~ 0.07 Å) in the fractional coordinate. The shift along the b axis is comparable with that of the RT structure. Figure 3(c) shows the temperature dependence of the shift of the TDAE molecules along the c axis. It should be noted that the C=C double bond of C_{60} is aligned along the c axis only when the neighboring TDAE molecules along the b direction (Nos. 2, 4, 6, and 8 in Fig. 4) approach each other along the c direction, as shown in the figure. The molecular twofold axis of C_{60} is aligned
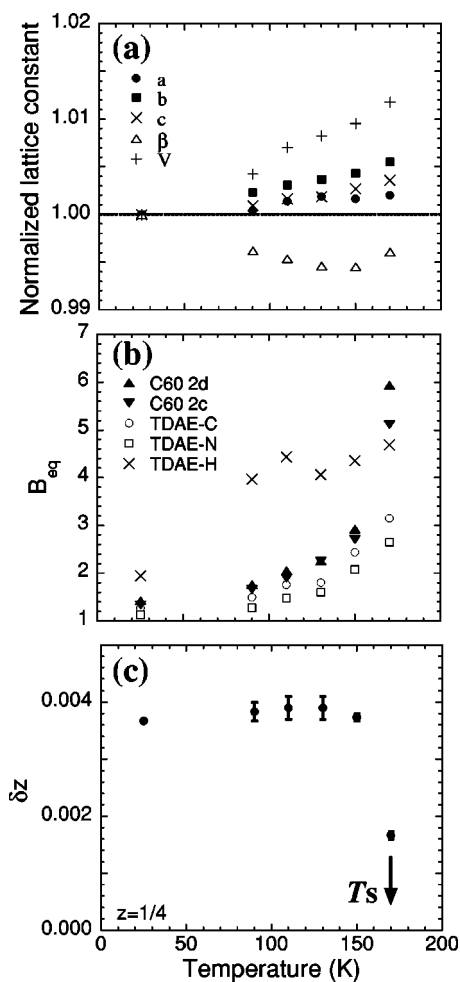

FIG. 3. (a) Temperature dependence of the lattice constants below T_s. The data are normalized by the data collected at 25 K. (b) Temperature dependence of the isotropic equivalent temperature factors B_{eq} averaged over the carbon atoms of the C_{60} molecule on $2c$ site (▼), the carbon atoms of the C_{60} molecule on $2d$ site (▲), the carbon atoms of the TDAE molecule (○), the nitrogen atoms of the TDAE molecule (□), and the proton atoms of the terminal methyl groups of the TDAE molecule (×). (c) Temperature dependence of the shift of the TDAE molecules along the c axis. TDAEs are placed on (~ 0, ~ 0.003, and $0.25 \pm \delta z$).

parallel to one of the C=C double bonds. This result clearly indicates that these shifts correlate to the alignment of the C_{60}s and that the steric effect between the C_{60} and TDAE molecules plays a key role in deciding the orientation of C_{60}. As shown in the figure, the TDAE molecules stack alternately along the c axis. In the low-temperature structure of the α phase, the C···C distances between the methyl groups in a TDAE pair are 4.520 Å and 4.840 Å along the c direction. The shift of the TDAE molecules along the c axis probably makes their dimerization tight. This may affect the spin cancellation of a TDAE pair.

Next, we comment on the valence states of a TDAE molecule in two phases. The central C=C double bond and the torsional angle ϕ in the N_2C-CN_2 fragment of a TDAE molecule are sensitive to the charge state of the molecule.[12,13] Using structural parameters, the C=C lengths are 1.413 and

TABLE III. Atomic coordinates and B_{iso}/B_{eq} for the C_{60} molecules of the α phase.

Atom	x	y	z	B_{eq}
C(1)	0.6308(2)	−0.0918(3)	−0.1246(2)	1.52(7)
C(2)	0.5925(2)	0.0928(3)	−0.1459(2)	1.56(7)
C(3)	0.6524(2)	0.0205(3)	−0.1216(2)	1.36(7)
C(4)	0.5507(2)	−0.1232(3)	−0.1518(2)	1.42(7)
C(5)	0.5830(2)	0.1899(2)	−0.1071(2)	1.60(8)
C(6)	0.6694(2)	−0.1408(3)	−0.0651(2)	1.59(7)
C(7)	0.5426(2)	−0.2526(2)	−0.0608(2)	1.15(7)
C(8)	0.5049(2)	−0.2056(2)	−0.1191(2)	1.27(7)
C(9)	0.5099(2)	0.0613(3)	−0.1737(2)	1.54(7)
C(10)	0.6261(2)	−0.2199(2)	−0.0336(2)	1.19(7)
C(11)	0.4894(2)	−0.0453(3)	−0.1768(2)	1.67(8)
C(12)	0.7035(2)	0.0369(3)	−0.0592(2)	1.63(7)
C(13)	0.4941(2)	0.2159(2)	−0.1129(2)	1.48(7)
C(14)	0.7150(2)	−0.0609(3)	−0.0232(2)	1.45(7)
C(15)	0.4479(2)	0.1365(3)	−0.1538(2)	1.63(8)
C(16)	0.4922(2)	−0.2760(2)	−0.0044(2)	1.11(7)
C(17)	0.4153(2)	−0.1801(2)	−0.1241(2)	1.24(7)
C(18)	0.6267(2)	−0.2235(2)	0.0406(2)	1.39(7)
C(19)	0.4053(2)	−0.0799(3)	−0.1601(2)	1.60(8)
C(20)	0.5432(2)	−0.2581(2)	0.0582(2)	1.29(7)
C(21)	0.7148(2)	−0.0660(2)	0.0464(2)	1.46(7)
C(22)	0.4052(2)	−0.2509(2)	−0.0096(2)	1.2433
C(23)	0.3675(2)	0.1041(2)	−0.1370(2)	1.37(7)
C(24)	0.3665(2)	−0.2024(2)	−0.0703(2)	1.36(7)
C(25)	0.6700(2)	−0.1474(2)	0.0798(2)	1.46(7)
C(26)	0.3464(2)	−0.0072(3)	−0.1407(2)	1.62(8)
C(27)	0.3054(2)	−0.1259(2)	−0.0506(2)	1.05(7)
C(28)	0.2961(2)	−0.0306(3)	−0.0852(2)	1.54(7)
C(29)	0.3681(2)	−0.2064(2)	0.0486(2)	1.50(7)
C(30)	0.3050(2)	−0.1279(3)	0.0221(2)	1.59(7)
C(31)	0.5646(2)	−0.0346(3)	0.6741(2)	1.47(7)
C(32)	0.6188(2)	−0.1020(3)	0.6447(2)	1.42(7)
C(33)	0.4746(2)	−0.0567(3)	0.6718(2)	1.46(7)
C(34)	0.5858(2)	−0.1965(2)	0.6122(2)	1.28(7)
C(35)	0.4985(2)	−0.2188(2)	0.6099(2)	1.20(7)
C(36)	0.4420(2)	−0.1465(3)	0.6406(2)	1.50(7)
C(37)	0.4278(2)	0.0412(3)	0.6627(2)	1.40(7)
C(38)	0.6858(2)	−0.0615(3)	0.6050(2)	1.40(7)
C(39)	0.6316(2)	−0.2139(2)	0.5530(2)	1.30(7)
C(40)	0.4551(2)	−0.2587(2)	0.5493(2)	1.26(7)
C(41)	0.3514(2)	0.0435(3)	0.6222(2)	1.23(7)
C(42)	0.3619(2)	−0.1438(2)	0.5980(2)	1.37(7)
C(43)	0.6937(2)	−0.1312(2)	0.5486(2)	1.07(7)
C(44)	0.3335(2)	0.1311(2)	0.5758(2)	1.29(7)
C(45)	0.3701(2)	−0.2134(2)	0.5407(2)	1.17(7)
C(46)	0.5895(2)	−0.2533(2)	0.4938(2)	1.1903
C(47)	0.4991(2)	−0.2759(2)	0.4917(2)	1.2025
C(48)	0.3180(2)	−0.0502(2)	0.5888(2)	1.46(7)

TABLE III. (*Continued.*)

Atom	x	y	z	B_{eq}
C(49)	0.2899(2)	0.0917(3)	0.5147(2)	1.37(7)
C(50)	0.2803(2)	−0.0223(3)	0.5227(2)	1.34(7)
C(51)	0.3338(2)	−0.1858(2)	0.4771(2)	1.51(7)
C(52)	0.6069(2)	−0.2110(2)	0.4277(2)	1.29(7)
C(53)	0.4604(2)	−0.2481(2)	0.4253(2)	1.30(7)
C(54)	0.2874(2)	−0.0868(2)	0.4671(2)	1.31(7)
C(55)	0.3790(2)	−0.2035(2)	0.4179(2)	1.46(7)
C(56)	0.5266(2)	−0.2073(2)	0.3853(2)	1.33(7)
C(57)	0.3053(2)	−0.0451(3)	0.4027(2)	1.53(7)
C(58)	0.3619(2)	−0.1166(2)	0.3710(2)	1.28(7)
C(59)	0.5100(2)	−0.1234(3)	0.3409(2)	1.43(7)
C(60)	0.4256(2)	−0.0781(3)	0.3336(2)	1.39(7)

1.419 Å in the α and α' phases, respectively. Further, the torsional angle $\phi(N_2C\!\!=\!\!CN_2)$ is also 116° in both phases. Comparing the molecular orbital (MO) calculations,[12,13] the TDAE molecules in the α and α' phases exist as monovalent cations, indicating that TDAE has a $S = 1/2$ spin. Therefore, the structural difference between the two phases barely affects the valence state of the TDAE molecules.

The existence of the structural phase transition in the α phase is in good agreement with the other experiments. Highly asymmetric ^{13}C nuclear magnetic resonance (NMR) spectra, in which the carbon atoms on C_{60} are enriched, were observed below 160 K; further, a broadening of the linewidths was observed.[14] They discussed the broadening in relation to the dynamical transition in the rotational motion of C_{60}. However, below 160 K, two correlation times for the rotational dynamics of C_{60} increased by more than 2 orders of magnitude. It can be assumed that this NMR behavior is due to the static ordering of the rotational dynamics of C_{60} below the observed structural phase transition. Furthermore, the temperature dependence of dc conductivity showed a clear discontinuity of slope at approximately 150 K.[15] These results indicate that the orientational ordering of C_{60} modulates the intermolecular overlap of electronic wave functions. The obtained activation energy decreased below this temperature, indicating the enhancement of the intermolecular contact due to the orientational ordering.

Our findings for the structural phase transition in the α phase seem to be consistent with these physical properties. However, the R factors in the two structural analyses (disorder model[10] and our model) are almost comparable. Which structural model is suitable to describe the low-temperature structure of the α phase? In the disorder model,[10] the intense superlattice reflections, which violate the extinction rules of the C-centered lattice, are perfectly excluded in the structural refinement because room-temperature space group symmetry ($C2/c$) was assumed. In that case, less than half of the observed reflections were used in the analysis. If we apply this method to our structural data, the R factor improves slightly to 4.8% when the ratio of the two configurations is approximately 55%/45%.[16] This ratio is comparable with the previous one.[10] Consequently, this leads to the absence of the

TABLE IV. Atomic coordinates and B_{iso}/B_{eq} for the TDAE molecules of the α phase.

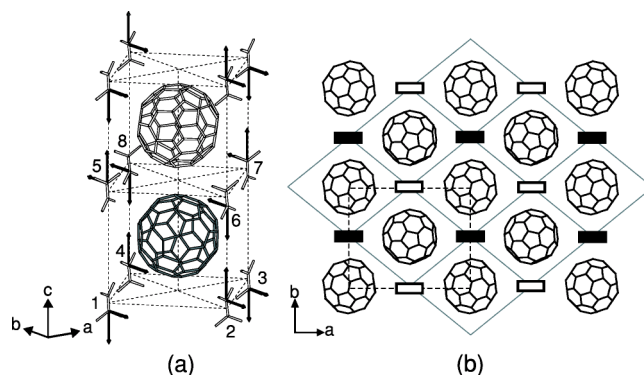| Atom	x	y	z	B_{eq}
N(1)	−0.0611(2)	−0.0289(2)	0.1731(1)	1.09(6)
N(2)	0.0759(2)	0.0409(2)	0.1940(1)	1.16(6)
N(3)	0.0613(2)	−0.0328(2)	0.3317(1)	1.10(6)
N(4)	−0.0785(2)	0.0305(2)	0.3155(2)	1.22(6)
C(61)	0.0031(2)	0.0051(2)	0.2182(2)	1.04(7)
C(62)	−0.0052(2)	0.0015(2)	0.2886(2)	1.00(7)
C(63)	−0.1243(2)	−0.1043(2)	0.1930(2)	1.16(7)
C(64)	−0.0789(2)	0.0197(3)	0.1070(2)	1.30(7)
C(65)	0.1144(2)	−0.0096(3)	0.1381(2)	1.46(7)
C(66)	0.1270(2)	0.1217(3)	0.2307(2)	1.52(7)
C(67)	0.1231(2)	−0.1064(2)	0.3079(2)	1.13(7)
C(68)	0.0824(2)	0.0150(2)	0.3977(2)	1.24(7)
C(69)	−0.1101(2)	−0.0228(3)	0.3733(2)	1.39(7)
C(70)	−0.1345(2)	0.1104(3)	0.2831(2)	1.48(7)
H(1)	−0.097(2)	−0.149(2)	0.234(2)	0.3(4)
H(2)	−0.178(3)	−0.070(3)	0.207(2)	2.5(6)
H(3)	−0.142(2)	−0.153(3)	0.151(2)	1.9(6)
H(4)	−0.138(3)	0.062(3)	0.108(2)	2.8(7)
H(5)	−0.085(2)	−0.037(3)	0.073(2)	1.8(6)
H(6)	−0.029(2)	0.064(3)	0.098(2)	1.6(5)
H(7)	0.075(3)	−0.069(4)	0.117(2)	3.1(7)
H(8)	0.121(3)	0.040(4)	0.097(2)	3.5(7)
H(9)	0.177(3)	−0.037(3)	0.157(2)	2.9(7)
H(10)	0.152(3)	0.170(3)	0.196(2)	2.4(6)
H(11)	0.179(3)	0.092(3)	0.261(2)	2.3(6)
H(12)	0.089(3)	0.162(3)	0.263(2)	2.3(6)
H(13)	0.097(2)	−0.154(3)	0.270(2)	0.4(4)
H(14)	0.174(2)	−0.071(2)	0.287(2)	1.7(6)
H(15)	0.147(2)	−0.152(3)	0.350(2)	1.3(5)
H(16)	0.142(3)	0.055(3)	0.399(2)	2.9(7)
H(17)	0.091(2)	−0.040(3)	0.437(2)	1.1(5)
H(18)	0.035(2)	0.062(3)	0.408(2)	1.8(6)
H(19)	−0.070(2)	−0.078(3)	0.388(2)	1.2(5)
H(20)	−0.114(2)	0.024(3)	0.415(2)	1.1(5)
H(21)	−0.171(3)	−0.050(3)	0.359(2)	2.4(6)
H(22)	−0.154(3)	0.158(3)	0.321(2)	2.5(6)
H(23)	−0.189(3)	0.079(3)	0.259(2)	2.2(6)
H(24)	−0.105(2)	0.148(3)	0.247(2)	0.7(5)

FIG. 4. Correlation between the shift of the TDAE molecules and the alignment of C_{60} in the low-temperature phase of ferromagnetic α-phase crystals. (a) Shift of the TDAE molecules along the b and c axes, indicated by thick arrows. (b) Alignment of C_{60} molecules viewed from the c axis. Open (closed) rectangles represent the TDAE molecules at $z=0.25+0.004$ ($z=0.25-0.004$).

hibits no structural phase transition and no ferromagnetic behavior.[5] The lower symmetry permits the shift of the TDAE molecules along the c direction and leads to the existence of two inequivalent C_{60} sites. Although the reasons for the absence of the phase transition and the restriction of the TDAE molecules in the α' phase are not clear at present, the structural differences distinguish the magnetic peculiarities of the two polymorphs in TDAE-C_{60}. Similar "orbital" ordering, which greatly controls the magnetism, has been observed in the ammoniated alkali C_{60} salt $NH_3K_3C_{60}$.[17–19] It is proposed that the antiferrorotative (ferrorotative) ordering leads to the ferromagnetic (antiferromagnetic) interaction between the spins on C_{60}. Structurally, at least two inequivalent C_{60} sites should exist in order to introduce the ferromagnetic intermolecular interactions. Two possible orientational ordering patterns in the low-temperature phase of α-TDAE-C_{60} are presented in Fig. 5, in which the JT-distorted C_{60} is described by the ellipse. These examples are consistent with the symmetry of the low-temperature structure. In Fig. 5(a), one of the JT axes of C_{60}s aligns parallel to the c axis and the other is parallel to the ab plane, while in (b), the axes align alternatively within the ab plane. In both cases, the orienta-
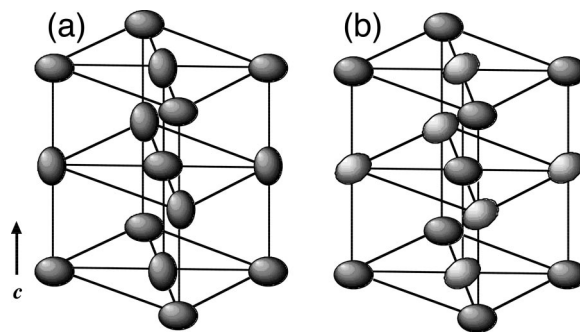

FIG. 5. Possible orientational ordering pattern in the low-temperature phase of α-TDAE-C_{60}. The Jahn-Teller distorted C_{60}s are depicted by the ellipse. (a) The elongated axes of C_{60}s are aligned parallel to the c axis and ab plane alternatively. (b) The axes are aligned within the ab plane.

shift of TDAE molecules along the c axis. The contact configuration of C_{60} along the c axis in our analysis is the same as the FM I-II configuration.[10] Although the R factor may improved slightly, these superlattice reflections cannot be strictly ignored (in the disorder model, the R factor for these superlattice reflections must be 1). We emphasize that our model was directly solved without any special assumption and was refined.

The structural phase change possibly guides the ferromagnetic transition of TDAE-C_{60} since the α'-phase crystal ex-

tions of C_{60} are ordered antiferrorotatively along the [001] and [110] directions. These directions correspond to the next nearest contact between the C_{60}s. Therefore, it is expected that intermolecular ferromagnetic interaction is induced along these directions. Since TDAE molecules exist between the C_{60} molecules along the [100] and [010] directions, the intermolecular interactions along these directions would be indirect, which may cause superexchange-type antiferromagnetic correlations to exist. Recently, ESR measurements under uniaxial pressure were conducted by Mizoguchi et al.[20] It is interesting to note that in their study, the ferromagnetic transition temperature strongly depended on the direction of the uniaxial pressure against the crystal axes. They proposed the orbital ordering pattern shown in Fig. 5(a) because of the rapid decline in T_c by the uniaxial strain along the c axis. This is because the intermolecular transfer along the c axis would be effectively modulated by such a strain. Their finding strongly supports our low-temperature structure for ferromagnetic α-TDAE-C_{60}.

IV. CONCLUSION

In summary, we have examined the x-ray diffraction measurements of several single crystals of the ferromagnetic α phase as well as the nonferromagnetic α' phase of TDAE-C_{60}. We observed the following structural peculiarities in the two polymorphs of TDAE-C_{60}: (1) The structural phase transition occurs in the α phase at 170 K while the α' phase holds the same structural symmetry as that of a RT structure below 25 K. (2) Two inequivalent C_{60} sites exist in the α phase while in the α' phase, all the C_{60}s are equivalent. (3) The orientation of C_{60} is ordered at a low temperature in both the phases; however, the contact configurations along the c direction are different. (4) In the α phase, the surrounding TDAE molecules shift along the c direction below T_s. The orientation of C_{60} perfectly correlates to the shift of TDAE molecules. This structural difference at a low temperature has been clearly observed in the two polymorphs. The magnetism of TDAE-C_{60} strongly depends on the structural peculiarities and the degree of freedom of the orbitals of C_{60}, thus leading to a difference in the mixing of intermolecular wave functions among C_{60}s and between TDAE and C_{60}.

*Corresponding author; Email address: kambe@science.okayama-u.ac.jp

[1] See, for example, *Molecular Magnetism* edited by O. Kahn (Wiley-VCH, New York, 1993).

[2] P. M. Allemand, K. C. Khemani, A. Koch, F. Wudl, K. Holczer, S. Donovan, G. Gruner, and J. D. Thompson, Science **253**, 301 (1991).

[3] D. Arcon, P. Cevc, A. Omerzu, and R. Blinc, Phys. Rev. Lett. **80**, 1529 (1998).

[4] Z. Jaglicic, Z. Trontelj, J. Pirnat, and R. Blinc, Solid State Commun. **101**, 591 (1997).

[5] D. Arcon, R. Blinc, P. Cevc, and A. Omerzu, Phys. Rev. B **59**, 5247 (1999).

[6] T. Kawamoto, Solid State Commun. **101**, 231 (1997).

[7] S. Garaj, T. Kambe, L. Forro, A. Sienkiewicz, M. Fujiwara, and K. Oshima, Phys. Rev. B **68**, 144430 (2003); T. Kambe, M. Fujiwara, K. Oshima, S. Garaj, A. Shienkievicz, and L. Forro, Synth. Met. **133–134**, 697 (2003).

[8] K. Mizoguchi, M. Machino, H. Sakamoto, T. Kawamoto, M. Tokumoto, A. Omerzu, and D. Mihailovic, Phys. Rev. B **63**, 140417 (2001).

[9] T. Kambe, Y. Nogami, and K. Oshima, Phys. Rev. B **61**, R862 (2000).

[10] B. Narymbetov, A. Omerzu, V. V. Kabanov, M. Tokumoto, H. Kobayashi, and D. Mihailovic, Nature (London) **407**, 883 (2000) and supplementary information ⟨http:www.nature.com⟩

[11] B. Narymbetov, H. Kobayashi, M. Tokumoto, A. Omerzu, and D. Mihailovic, Chem. Commun. (Cambridge) **16**, 1511 (1999).

[12] K. I. Pokhodnia, J. Papavassiliou, P. Umek, A. Omerzu, and D. Mihailovic, J. Chem. Phys. **110**, 3606 (1999).

[13] S. Hino, K. Umishita, K. Iwasaki, K. Tanaka, T. Sato, T. Yamabe, K. Yoshizawa, and K. Okahara, J. Phys. Chem. A **110**, 4346 (1997).

[14] P. Jeglic, R. Blinc, T. Apih, A. Omerzu, and D. Arcon, Phys. Rev. B **68**, 184422 (2003).

[15] A. Omerzu, D. Mihailovic, S. Tomic, O. Milat, and N. Biskup, Phys. Rev. Lett. **77**, 2045 (1996).

[16] M. Fujiwara, PhD thesis, Okayama University, 2005.

[17] K. Ishii, T. Watanuki, A. Fujiwara, H. Suematsu, Y. Iwasa, H. Shimoda, T. Mitani, H. Nakao, Y. Fujii, Y. Murakami, and H. Kawada, Phys. Rev. B **59**, 3956 (1999).

[18] H. Tou, Y. Maniwa, Y. Iwasa, H. Shimoda, and T. Mitani, Phys. Rev. B **62**, R775 (2000).

[19] S. Margadonna, K. Prassides, H. Shimoda, T. Takenobu, and Y. Iwasa, Phys. Rev. B **64**, 132414 (2001).

[20] K. Mizoguchi, M. Takei, M. Machino, H. Sakamoto, M. Tokumoto, T. Kawamoto, A. Omerzu, and D. Mihailovic, J. Magn. Magn. Mater. **272–276**, E215 (2004); (private communication).